Quantum computation with moving quantum dots generated by surface acoustic waves

X. Shi, M. Zhang, and L. F. Wei

Phys. Rev. A **84**, 062310 — Published 15 December 2011

DOI: 10.1103/PhysRevA.84.062310

Quantum computation with moving quantum dots generated by surface acoustic waves

X. Shi,[1] M. Zhang,[1] and L. F. Wei*[1,2]

[1]*Quantum Optoelectronics Laboratory, School of Physics and Technology, Southwest Jiaotong University, Chengdu 610031, China*

[2]*State Key Laboratory of Optoelectronic Materials and Technologies, School of Physics Science and Engineering, Sun Yet-sen University, Guangzhou 510275, China*

Abstract

Motivated by the recent experimental observations [M. Kataoka et al., Phys. Rev. Lett. **102**, 156801 (2009)], we propose here an theoretical approach to implement quantum computation with bound states of electrons in moving quantum dots generated by the driving of surface acoustic waves. Differing from static quantum dots defined by a series of static electrodes above the two-dimensional electron gas (2DEG), here a single electron is captured from a 2DEG-reservoir by a surface acoustic wave (SAW) and then trapped in a moving quantum dot (MQD) transported across a quasi-one dimensional channel (Q1DC), wherein all the electrons have been excluded by the actions of the surface gates. The flying qubit introduced here is encoded by the two lowest levels of the electron in the MQD, and the Rabi oscillation between these two levels could be implemented by applying finely-selected microwave pulses to the surface gates. By using the Coulomb interaction between the electrons in different MQDs, we show that a desirable two-qubit operation, i.e., i-SWAP gate, could be realized. Readouts of the present flying qubits are also feasible with the current single-electron detected technique.

PACS numbers: 73.50.Rb, 73.63.Kv, 03.67.Lx, 73.23.Hk.

* weilianfu@gmail.com

I. INTRODUCTION

In the past decades a considerable attention is paid to quantum computation implemented usually by an array of weakly-coupled quantum systems [1]. Basically, a quantum computing process involves a series of time-evolutions of the coupled two-level quantum systems (qubits). In the classical computer, the information unit is represented by a bit, which is always understood as either 0 or 1. The information unit in quantum computation is very different. For example, the qubit can be at logic "0" or logic "1" and also the superposition of both. Owing to this property, quantum computer provides an automatically-parallel computing and thus possesses much more powerful features than that realized by the classical computer. This basic advantage has been definitely demonstrated with Shor algorithm [2] for significantly speeding up the large number factoring.

A central challenge in the current quantum information science is, how to build such a quantum computer? Until now, there has been many proposals for experimental quantum computation, such as atomic qubits coupled via a cavity field [3, 4], cold ions confined in a linear trap [5], nuclear magnetic resonance [6], photons [7, 8], quantum dots [9, 10], and Josephson superconducting system [11], etc.. Note that all these candidates are based on the static qubits, and the controllable interbit interactions are difficult to achieve. Alternatively, in this paper we focus on the flying qubits generated by the electrons in moving quantum dots (MQDs). In fact, quantized transport of electrons along a quasi-one dimensional channel (Q1DC) by surface acoustic waves have been observed [12, 13]. The original attempt in these experiments is to build the desirable current standards, but now has also leaded to the study of quantum computation. The qubit in such a systems is "flying" [14, 15], since the electron in the MQD is drawn along the Q1DC by a surface acoustic wave (SAW). In principle, quantum computing with these flying qubits realized by using SAWs possess two manifest advantages [16, 17]: i) one can make ensemble measurements over billions of identical MQDs and thus be robust against various random errors, and ii) it should allow a longer quantum operation by preventing the spreading of the wave function and reducing undesired reflection effects.

The approach using the above SAW-based flying qubits to implement quantum computation was first proposed by Barnes et al [14], who used two spin-states of the transported electron to encode a flying qubit. Although the feasibility of this proposal was then analyzed in detail [15], the experimental demonstration of this proposal has not been achieved yet. One of the possible obstacles is that the required local magnetic fields are not easy to apply for manipulating the spin-

states of the electrons in the MQDs. In order to overcome such a difficulty, the flying qubits in our quantum computing proposal are directly encoded by the two bound-states (rather than the above spin-states) of the electrons in the MQDs. In principle, there are a few electronic levels within each MQD, but only the two lowest ones with relatively-long lifetimes are suitably selected to encode a qubit. Our idea is motivated by the recent experimental work, wherein the coherent single-electron dynamics on these bound states was successfully observed [18].

The paper is organized as follows. In Sec. II we briefly describe the SAW-based MQDs and numerically calculate the electronic levels. How these levels change adiabatically during the MQD transporting along the Q1DC are also discussed. By applying an additional driving electric field to the gates above the channel, we show in Sec. III that the Rabi oscillations between the qubit's levels could be implemented. In Sec. IV, we describe an approach to implement a two-qubit operation between the flying qubits across different channels. Finally, we summarize our main results and give some discussions on feasibility of our proposal, including how to read out the proposed flying qubit by using the existing experimental-technique.

II. SAW-BASED MOVING QUANTUM DOTS

We consider the system demonstrated first to experimentally observe quantized-acoustoelectric-currents [18–21]. A two-dimensional electron gas (2DEG) is formed in a GaAs/AlGaAs heterostructure below the metallic surface split-gate. At $1.5\ K$ the electronic density and the mobility in this 2DEG are measured as [20] $1.8 \times 10^{15}\ m^{-2}$ and $160\ m^2V^{-1}s^{-1}$, respectively. The surface gates are utilized to define a Q1DC without any electron. Two SAW interdigital transducers placed on each side of the device are used to generate a SAW (with a resonant frequency around $3\ GHz$) propagating along the Q1DC. The surface gate geometry is chosen to produce an electrostatically defined channel with the length approximately of the SAW wavelength ($\lambda = 1\ \mu$m), so that a single electron can be periodically transported through the channel. The moving potential containing only one electron can serve as a MQD. Of course, when the quantum dot carrying few electrons moves through the channel, a quantized current is generated. This current can be measured by connecting an ammeter to two Ohmic contacts on the 2DEG mesa.

For simplicity, we assume that only one electron is captured into the MQD and then propagates along the narrow depleted Q1DC. The potential of the electron in a MQD could be effectively

simplified as

$$V_{\rm eff}(z,t) = V_{\rm SAW}(z,t) + V_{\rm gate}(z), \tag{1}$$

where $V_{\rm SAW}(z,t)$ and $V_{\rm gate}(z)$ are the piezoelectric potential accompanying the SAW and the electrostatic potential defined by the surface split-gate, respectively. First, the thickness and width of the quantum dot (i.e., its sizes along the y- and x-direction) are all neglected, such that the electrostatic potential could be simply modeled as a strictly 1D potential [22, 23]

$$V_{\rm gate}(z) = \frac{V_0}{\cosh^2(z/a)}. \tag{2}$$

Here, the z-axis is chosen along the channel which the SAW propagates through and the parameter V_0 determines the effective height of the potential barrier. The split-gate is operated well beyond the pinch off voltage in the absence of the SAW, so the energy V_0 could be greater than the electron Fermi energy in the 2DEG, and the edge of the depleted Q1DC is well away from the edge of the surface split-gate. The effective length of the Q1DC can be taken as $l_{\rm eff} = 2a$, and it takes also approximately as long as the SAW wavelength $\lambda(= 1\,\mu{\rm m})$. Consequently, we have $a = 0.5\ \mu$m. Next, by considering the screening effect of the metal gates on the SAW-induced electric potential, and neglecting the mechanical coupling between the semiconductor and the metal surface gate, all the changes in the components of the stress tensor, and the separation between split-gates, etc., Aĭzin $et\ al$ [24] showed that the piezoelectric potential $V_{\rm SAW}$ could be simplified to the form

$$V_{\rm SAW} = V_S \cos(kz - wt). \tag{3}$$

Here, V_S is the amplitude of the SAW, and k and w are the frequency and wave number, respectively.

With the above potential the electronic levels of the electron trapped in the MQD can be determined by solving the instantaneous eigenvalue equation

$$\begin{aligned} &\hat{H}_0(t)|E_n(t)\rangle = E_n(t)|\psi_n(t)\rangle, \\ &\hat{H}_0(t) = -\frac{\hbar^2}{2m^*}\frac{d^2}{dz^2} + \frac{V_0}{\cosh^2(z/a)} + V_S\cos(kx - wt). \end{aligned} \tag{4}$$

Here, $m^* = 0.0067m_e$ is the effective mass of the electron in GaAs, and $V_0 = \hbar^2/2m^*l_0^2$, $V_S = \gamma V_0$. The parameter $l_0 = 4\times10^{-2}a$ is the effective width of the Q1DC, and $\gamma = 0.5$ the ratio of the SAW potential amplitude to the height of the electrostatically-induced potential barrier in the Q1DC. The SAW velocity is $v = 2981$ m/s [22]. By finite differential method we can numerically

solve Eq. (4) and obtain the electronic levels in the MQD. Although the shape of the potential or the size of the quantum dot changes with the motion, the dot is still "big" enough to hold a few levels. Specifically, Fig. 2 shows the effective potential and its corresponding bound levels

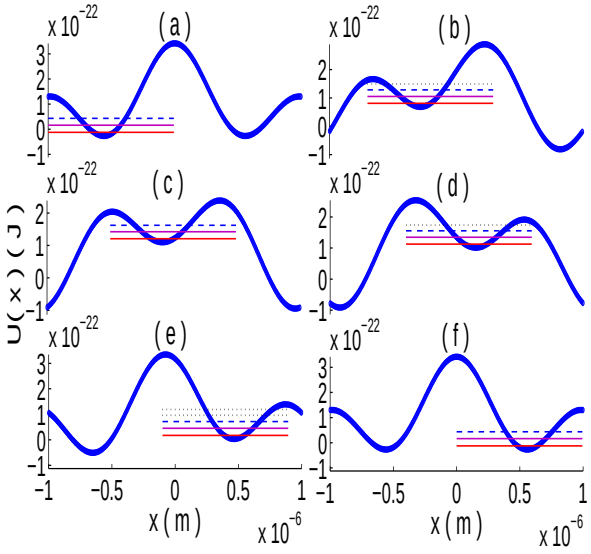

FIG. 1: (Color online) The effective potential and its allowed energy levels for $\gamma = 0.5$ at various typical times: (a) $t = 0$ ns, (b) $t = 0.1$ ns, (c) $t = 0.15$ ns, (d) $t = 0.2$ ns, (e) $t = 0.3$ ns, and (f) $t = T = 0.34$ ns. The blue solid line represents the effective potential and the colored lines show the allowed levels: ground state (lower red line), the first exited state (upper purple line), the second excited state (dashed blue line), the other excited state (dotted black line).

for the different times over the SAW period. Qualitatively, the dot could capture many electrons initially, but most of them will be escaped from the local well and returned to the source reservoir. In the present calculation, we consider the ideal condition wherein only one electron is initially captured by the MQD and held in where across the channel. One can see from Fig. 2 that, a few bound levels exist in the local potential of the quantum dot moving along the channel. A snapshot of the wave function and the corresponding probabilistic distributions of the electron residing in these levels in a specific moment are shown in Fig. 3. Indeed, our numerical calculations show clearly that only the electron in the third (dotted blue-line) level could escape from the well. We see specifically from Fig. 3(c) that, only the wave function of the third adiabatic levels had a (significantly) small probability for tunneling out the trapped potential. Such a tunneling wave function has really certain overlap with the adjacent potential, although the relevant probability is still sufficiently low, e.g., less than 6%. Therefore, such a tunneling is still negligible compared

with the probabilities of the lowest two levels in the adjacent potential. The higher adiabatic levels have the higher tunneling probabilities, but their original occupation probabilities are really very small and thus these tunnelings can be safely neglected. Typically, the probabilities of the electron in the lowest two levels, the ground and first excited ones, tunneling to the source reservoir is negligible. In other times, there may be more levels in the local well as shown in Fig. 2, although we don't emerge these levels out in Fig. 3, but certainly two lowest levels with relatively-long lifetimes are suitably selected to encode the desirable flying qubit, the unit of the moving quantum information.

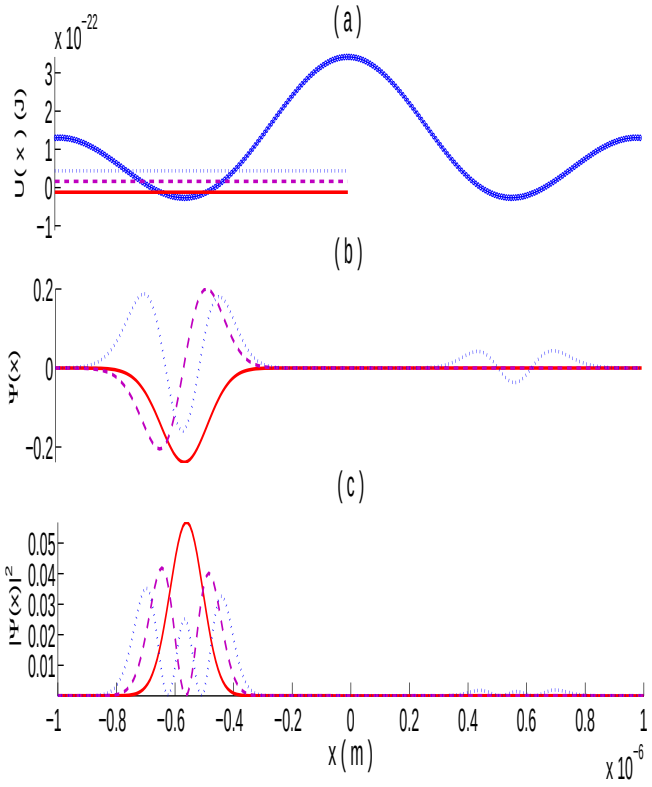

FIG. 2: (Color online) Wave functions of the lowest three levels and their relevant probabilistic distributions at certain time (with the maximum tunneling probability): (a) Potential and its allowed levels, (b) The eigen-functions of the allowed levels and (c) the probabilistic distributions of the electron in the allowed-levels along the channel. Here, the thick blue reveal the change of the potential, and the lower red, upper dashed purple and dotted blue lines denote the ground, the first excited and the second excited state, respectively.

We now show that the flying qubit defined above is sufficiently stationary, although the shape

of the potential varies with the quantum dot moving along the channel. The adiabatic theorem asserts that, if the rate of the change of Hamiltonian is slow enough, the system will stay at an instantaneous eigenstate of the time-Hamiltonian. For the present case the adiabatic condition is expressed as

$$\beta = \left| \frac{\hbar \langle m| \frac{\partial H_0(t)}{\partial t} |n\rangle}{(E_m(t) - E_n(t))^2} \right| \ll 1, \tag{5}$$

where $E_m(t) - E_n(t)$ is the energy splitting between the state $|m\rangle$ and $|n\rangle$. Our numerical results show that, at certain time: $E_0 = -1.22 \times 10^{-23}\ J, E_1 = 1.64 \times 10^{-23}\ J$ and consequently $\beta = 0.0847$. This indicates that the adiabatic condition could be satisfied. A lower value of the β-parameter is also possible by properly adjusting the relevant parameters. This means that the levels used above to encode the flying qubit is adiabatic, and thus one can call them later as the so-called adiabatic levels. Thus, once the flying qubit is prepared at one of its logic states ($|0\rangle$ and $|1\rangle$), it always stays at that state until the specific driving is applied.

III. RABI OSCILLATIONS BETWEEN THE LEVELS OF FLYING QUBIT

For realizing quantum computation, we need to first implement arbitrary rotations of the single-qubit. For the present flying qubit, this can be achieved by using the usual Rabi oscillations between the adiabatic states $|0\rangle$ and $|1\rangle$. Basically, these states should be kept as the pure ones. This can be realized by cooling the system to a sufficiently low temperature $T_{\rm temp}$, such that the condition $k_B T_{\rm temp} \ll \hbar\omega$ is satisfied. Here, $\omega = \omega_1 - \omega_0$ is the electronic transition frequency of the flying qubit, and k_B is Boltzmann constant. Experimentally [18], the system can be worked approximately at the temperature $T_{\rm temp} = 0.27\ K$, yielding $k_B T_{\rm temp} = 3.726 \times 10^{-24}\ J \ll \hbar\omega \sim 2.8502 \times 10^{-23}\ J$. Thus, the transitions between the qubit's levels due to the thermal excitations can be safely neglected.

We now apply a resonant electric driving to the surface gates for implementing the desirable Rabi oscillations. Under such a driving the previous 1D-potential $V_{\rm gate}$, i.e., Eq. (2), is now changed as $V_{\rm gate} \to V'_{\rm gate} = V_{\rm gate} + V_e \cos(\omega t - \phi)/\cosh^2(z/a)$ with ω and ϕ being the frequency and initial phase of the driving field, respectively. Consequently, the dynamics of the driven flying qubit is determined by the following time-dependent Schrödinger equation

$$i\hbar \frac{\partial |\psi(t)\rangle}{\partial t} = (\hat{H}_0 + \hat{H}'(t,\phi))|\psi(t)\rangle. \tag{6}$$

with

$$\hat{H}'(t,\phi) = \frac{V_e \cos(\omega t - \phi)}{\cosh^2(z/a)}, \tag{7}$$

Above, V_e is a parameter depending on the power of the applied electric-filed. In our calculation, we choose it as $V_e = 0.3V_S$ for simplicity. Generally, the wave function of the driven flying qubit can be written as

$$|\psi(t)\rangle = C_0(t)|0\rangle + C_1(t)|1\rangle, \tag{8}$$

with $C_0(t)$ and $C_1(t)$ being the time-dependent probability-amplitudes of finding the electron in the states $|0\rangle$ and $|1\rangle$ at the time t, respectively.

From Eqs. (6-8), the equations of motion for the amplitudes $C_0(t)$ and $C_1(t)$ can be derived as

$$\frac{\partial C_0(t)}{\partial t} = -i\omega_0 C_0(t) - iC_0(t)D_{00}\cos(\omega t - \phi) - iC_1(t)D_{01}\cos(\omega t - \phi), \tag{9}$$

and

$$\frac{\partial C_1(t)}{\partial t} = -i\omega_1 C_1(t) - iC_1(t)D_{11}\cos(\omega t - \phi) - iC_0(t)D_{10}\cos(\omega t - \phi), \tag{10}$$

with $D_{ij} = V_e/[\hbar\langle i|\cosh^2(z/a)|j\rangle]$, $i,j = 0,1$. The method to solve the above ordinary differential equations is relatively-standard, e.g., by the existing program in Matlab software. Certainly, the relation

$$|C_0(t)|^2 + |C_1(t)|^2 = 1, \tag{11}$$

is always satisfied. With the initial condition $|\psi(0)\rangle = |0\rangle$ and $\phi = 0$ for simplicity, we plot the how the dynamical variable $|C_1(t)|^2$ changes with the time in Fig. 4. It is seen really that the population in one of the logic state of the flying reveals an obviously oscillating behavior with a period: $\tau \sim 0.31$ ns. This time-interval is sufficiently-long for the MQD across the Q1DC demonstrated in the experiment. The time interval for a quantum dot across the channel is estimated as $\sim 0.34\, ns$. Thus, Rabi oscillations between the levels $|0\rangle$ and $|1\rangle$ can be really demonstrated in the present MQD system.

Rabi oscillations are formally equivalent to the single-qubit σ_x operations: $|0\rangle \to |1\rangle$, $|1\rangle \to |0\rangle$. In principle, arbitrary single-qubit operation can be implemented by the combinations of a pair of noncommutable single-qubit operations [25] , e.g., σ_x and the phase-flip gate $\hat{U}(\theta) = \exp(i\theta)|0\rangle\langle 0| + \exp(-i\theta)|1\rangle\langle 1|$ generated by the free evolution of the qubit. However, if the initial phase ϕ of the driving field can be well defined, then the Hamiltonian of the driven qubit reads

$$\hat{H}(t,\phi) = H_0 + H'(t,\phi) \simeq \hbar\omega\hat{\sigma}_z + V_e\cos(\omega t - \phi)(1 - \frac{\hat{z}^2}{a^2}). \tag{12}$$

Above, the usual Taylor expansion is used and the high-order terms are neglected. Furthermore, the position operator $\hat{z}^2$ can be expressed (in the qubit's representation) as

$$\begin{aligned}\hat{z}^2 = &(z_{00}^2 + z_{01}z_{10})|0\rangle\langle 0| + (z_{11}^2 + z_{10}z_{01})|1\rangle\langle 1| \\ &+ (z_{00}z_{01} + z_{01}z_{11})|0\rangle\langle 1| + (z_{11}z_{10} + z_{10}z_{00})|0\rangle\langle 1|,\end{aligned} \tag{13}$$

where $z_{ij} = \langle i|z|j\rangle$ and $z_{ij} = z_{ji}$ $(i, j = 1, 2)$. Finally, in the interaction picture and under the usual rotating-wave approximation, the Hamiltonian of the driven qubit reduces to

$$\hat{H}_i = g\left(e^{-i\phi}|0\rangle\langle 1| + e^{i\phi}|1\rangle\langle 0|\right), \tag{14}$$

with $g = -V_e(z_{00}z_{01} + z_{01}z_{11})/(2a^2)$. This Hamiltonian yields the following arbitrary rotation

$$\hat{U}(\alpha, \phi) = \begin{pmatrix} \cos\alpha & -ie^{i\phi}\sin\alpha \\ -ie^{-i\phi}\sin\alpha & \cos\alpha \end{pmatrix}, \ \alpha = gt/\hbar, \tag{15}$$

of the qubit.

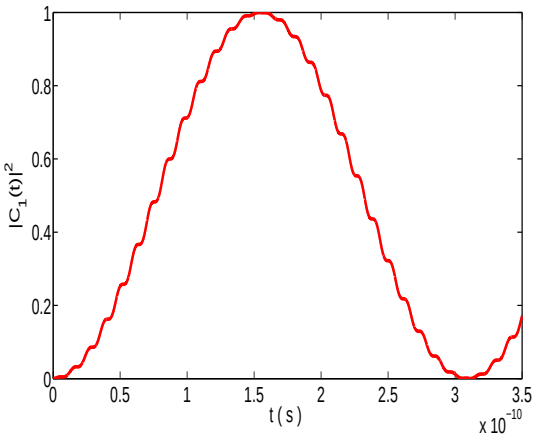

FIG. 3: (Color online) Rabi oscillation of the population in the qubit's level $|1\rangle$. The oscillation period shown here is about 0.31 ns. During a period time of the SAW 0.34 ns, if the electron is originally residing in the ground state, it could jump to the excited level $|1\rangle$ and then rotate to the initial state $|0\rangle$.

A problem may exist during the driving for implementing the desirable Rabi oscillation. That is, due to the adiabatic changes of the electronic levels the qubit's energy splitting changes adiabatically with the time. Consequently, it seems that the desirable Rabi oscillation implemented by usually applying a resonant pulse cannot be achieved. However, due to the adiabatic change of the energy splitting is practically weak, the qubit encoded by two adiabatic levels can always be

driven near-resonantly. In fact, within a very short time interval, the transition frequency changes very small. For example, when the interval is 0.01 ns, the change rate of the frequency is only 6.4% under the parameter chosen above. Thus, during a period time, the maximum change rate of the energy-splitting could be only 6% by properly setting the relevant parameter, e.g., for $\gamma = 2.2$. Under these near-resonant drivings, the desirable Rabi oscillations could still be achieved with the sufficiently-high fidelities. Therefore, the desirable Rabi oscillation could be achieved for the present qubit with slowly-changing energy-splitting, at least theoretically.

IV. COUPLING THE SEPARATED MOVING QUANTUM DOTS FOR TWO-FLYING-QUBIT OPERATIONS

We now discuss how to implement an universal gate, i.e., the two-qubit operation, with the MQDs. A simple way to achieve such a task is by utilizing the Coulomb interaction between the electrons in the nearest-neighbour interaction MQDs. To do this, let us consider the situation schematically shown in Fig. 5, wherein two MQDs driven by two SAWs pass across two Q1DCs, the upper- and lower ones. Suppose that the tunneling between them is negligible and only the Coulomb interaction between them is important. First, the Coulomb force between the electrons in these two MQDs can be expressed as

$$F_{\text{int}}(z_u, z_l) = \frac{e^2}{4\pi\varepsilon_0}\frac{(z_l - z_u)}{[d^2 + (z_l - z_u)^2]^{3/2}}, \tag{16}$$

with z_u and z_l being their coordinates along the channels (the indices u and l refer to the upper and lower channels, respectively) and d the distance between the two Q1DCs. Since the motions of the electrons are always along the Q1DCs, the vertical force of the Coulomb interaction can be ignored and thus only the horizontal force along the z-axis is taken account into. Second, the potential related to above force can be written as

$$V_{\text{int}}(z) = \frac{1}{4\pi\varepsilon_0}\int_0^z \frac{e^2 z dz}{(d^2 + z^2)^{3/2}} = -\frac{1}{4\pi\varepsilon_0}\frac{e^2}{d}\left\{\frac{1}{[1 + (z/d)^2]^{1/2}} - 1\right\}, \tag{17}$$

where $z = z_u - z_l$. By using the usual Taylor expansion and ignoring the high-order terms under the condition $d \gg z$, the above Coulomb potential reduces to

$$V_{\text{int}}(z) = \frac{e^2}{8\pi\varepsilon_0 d^3}z^2 = \frac{e^2}{8\pi\varepsilon_0 d^3}\left(z_u^2 + z_l^2 - 2z_u z_l\right). \tag{18}$$

Thirdly, the Hamiltonian describing the dynamics of the two-coupling MQDs reads

$$\hat{H}_h = \hat{H}_t + V_{\text{int}}(z), \tag{19}$$

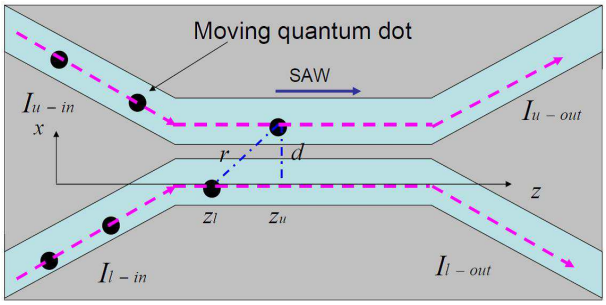

FIG. 4: (Color online) The schematic diagram to implement controllable couplings between two flying-qubits. Two MQDs passage along the the upper and lower Q1DCs, respectively, and the coupling between them is realized by the Coulomb interaction of the inside electrons. The z axis is chosen along the electronic path of the lower channel, and r is the distance between the upper electron and the lower one.

with

$$\hat{H}_t = \sum_{j=u,l}\left[-\frac{\hbar^2}{2m_j^*}\frac{d^2}{dz_j^2} + \frac{V_0^j}{\cosh^2(z_j/a)} + V_S^j\cos(kz_j-\omega t)\right] = \sum_{j=u,l}\frac{\hbar\omega_j}{2}\hat{\sigma}_j^z, \tag{20}$$

and $\hat{\sigma}_j^z = |1_j\rangle\langle 1_j| - |0_j\rangle\langle 0_j|$, $\omega_j = (E_1^j - E_0^j)/\hbar$.

In the qubit representation, the position operators $\hat{z}_j$, $\hat{z}_j^2$ and $\hat{z}_j\hat{z}_k$ (where $j,k = u,l$ and $j \neq k$) can be expressed as

$$\hat{z}_j = \frac{1}{2}(z_j^{11} - z_j^{00})\hat{\sigma}_j^z + z_j^{01}\hat{\sigma}_j^x,\ \ \hat{z}_j^2 = \frac{1}{2}(z_j^{11} + z_j^{00})(z_j^{11} - z_j^{00})\hat{\sigma}_j^z + (z_j^{00} + z_j^{11})z_j^{01}\hat{\sigma}_j^x, \tag{21}$$

and

$$\begin{aligned}\hat{z}_j\hat{z}_k = {} & \frac{1}{4}(z_k^{11} + z_k^{00})(z_j^{11} - z_j^{00})\hat{\sigma_j^z} + z_j^{01}z_k^{01}\hat{\sigma}_j^x\hat{\sigma}_k^x + \frac{1}{4}(z_j^{11} + z_j^{00})(z_k^{11} - z_k^{00})\hat{\sigma_k^z} \\ & + \frac{1}{2}(z_k^{00} + z_k^{11})z_j^{01}\hat{\sigma_j^x} + \frac{1}{2}(z_j^{00} + z_j^{11})z_k^{01}\hat{\sigma_k^x} + \frac{1}{4}(z_j^{11} - z_j^{00})(z_k^{11} - z_k^{00})\hat{\sigma_j^z}\hat{\sigma_k^z} \\ & + \frac{1}{2}(z_j^{11} - z_j^{00})z_k^{01}\hat{\sigma}_j^z\hat{\sigma}_k^x + \frac{1}{2}(z_k^{11} - z_k^{00})z_j^{01}\hat{\sigma}_j^z\hat{\sigma}_k^x,\end{aligned} \tag{22}$$

respectively. Above, $\hat{\sigma}_j^x = \hat{\sigma}_j^+ + \hat{\sigma}_j^-$ with $\hat{\sigma}_j^+ = |1_j\rangle\langle 0_j|$ and $\hat{\sigma}_j^- = |0_j\rangle\langle 1_j|$; z_j^{11}, z_j^{00} and z_j^{01} are the matrix elements $\langle 1_j|z_j|1_j\rangle$, $\langle 0_j|z_j|0_j\rangle$, and $\langle 1_j|z_j|0_j\rangle$, respectively. As a consequence, the above Coulomb potential $V_{\rm int}(z)$ can be rewritten as

$$\hat{V}_{\rm int} = C_u^z\hat{\sigma}_u^z + C_l^z\hat{\sigma}_l^z + C_u^x\hat{\sigma}_u^x + C_l^x\hat{\sigma}_l^x + C_{ul}^{zz}\hat{\sigma}_u^z\hat{\sigma}_l^z + C_{ul}^{xx}\hat{\sigma}_u^x\hat{\sigma}_l^x + C_{ul}^{zx}\hat{\sigma}_u^z\hat{\sigma}_l^x + C_{ul}^{xz}\hat{\sigma}_u^x\hat{\sigma}_l^z, \tag{23}$$

with

$$\begin{cases} C_u^z = \dfrac{e^2}{16\pi\varepsilon_0 d^3}(z_u^{00}+z_u^{11}-z_l^{00}-z_l^{11})(z_u^{11}-z_u^{00}), \\ C_l^z = \dfrac{e^2}{16\pi\varepsilon_0 d^3}(z_l^{00}+z_l^{11}-z_u^{00}-z_u^{11})(z_l^{11}-z_l^{00}), \\ C_u^x = \dfrac{e^2}{8\pi\varepsilon_0 d^3}(z_u^{00}+z_u^{11}-z_l^{00}-z_l^{11})z_u^{01}, \\ C_l^x = \dfrac{e^2}{8\pi\varepsilon_0 d^3}(z_l^{00}+z_l^{11}-z_u^{00}-z_u^{11})z_l^{01}, \end{cases}$$

and

$$\begin{cases} C_{ul}^{zz} = \dfrac{-e^2}{16\pi\varepsilon_0 d^3}(z_u^{11}-z_u^{00})(z_l^{11}-z_l^{00}),\ C_{ul}^{xx} = \dfrac{-e^2}{4\pi\varepsilon_0 d^3}z_u^{01}z_l^{01}, \\ C_{ul}^{zx} = \dfrac{-e^2}{8\pi\varepsilon_0 d^3}(z_u^{11}-z_u^{00})z_l^{01},\ C_{ul}^{xz} = \dfrac{-e^2}{8\pi\varepsilon_0 d^3}(z_l^{11}-z_l^{00})z_u^{01}. \end{cases}$$

In the interaction picture defined by the unitary $\hat{U}_0(t) = \exp\left[(-i/\hbar)t\sum_{j=u,l}\lambda_j\hat{\sigma}_j^z\right]$ with $\lambda_j = \hbar\omega_j/2 + C_j^z$, the Hamiltonian of the system reduces to

$$\begin{aligned} \hat{H}_I =& C_{ul}^{zz}\hat{\sigma}_u^z\hat{\sigma}_l^z + \sum_{j=u,l} C_j^x\left(e^{2it\lambda_j/\hbar}\hat{\sigma}_j^+ + e^{-2it\lambda_j/\hbar}\hat{\sigma}_j^-\right) \\ &+C_{ul}^{xx}\left[e^{2it(\lambda_u+\lambda_l)/\hbar}\hat{\sigma}_u^+\hat{\sigma}_l^+ + e^{2it(\lambda_u-\lambda_l)/\hbar}\hat{\sigma}_u^+\hat{\sigma}_l^- + e^{-2it(\lambda_u-\lambda_l)/\hbar}\hat{\sigma}_u^-\hat{\sigma}_l^+ + e^{-2it(\lambda_u+\lambda_l)/\hbar}\hat{\sigma}_u^-\hat{\sigma}_l^-\right] \\ &+C_{ul}^{zx}\left(e^{2it\lambda_l/\hbar}\hat{\sigma}_u^z\hat{\sigma}_l^+ + e^{-2it\lambda_l/\hbar}\hat{\sigma}_u^z\hat{\sigma}_l^-\right) + C_{ul}^{xz}\left(e^{2it\lambda_u/\hbar}\hat{\sigma}_u^+\hat{\sigma}_l^z + e^{-2it\lambda_u/\hbar}\hat{\sigma}_u^-\hat{\sigma}_l^z\right). \end{aligned} \tag{24}$$

Consequently, under the usual rotating-wave approximation, we have

$$\overline{H}_I = C_{ul}^{xx}(\hat{\sigma}_u^+\hat{\sigma}_l^- + \hat{\sigma}_u^-\hat{\sigma}_l^+). \tag{25}$$

During this derivation, the significantly-small quantities $C_{ul}^{zz} \ll C_{ul}^{xx}$ has been omitted, and we have also assumed that $\lambda_u = \lambda_l$. Typically, for the experimental parameters: $z = 2.981\times10^{-2}$ μm, we have $z_u^{00} = -5.3594\times10^{-1}$ μm, $z_u^{11} = -5.4418\times10^{-1}$ μm, $z_u^{01} = z_u^{10} = 5.6607\times10^{-2}$ μm; $z_l^{00} = -5.6186\times10^{-1}$ μm, $z_l^{11} = -5.6975\times10^{-1}$ μm, $z_l^{01} = z_l^{10} = -5.6431\times10^{-2}$ μm, and thus $|C_{ul}^{zz}/C_{ul}^{xx}| = 5.1\times10^{-3} \ll 1$.

Finally, the above Hamiltonian yield the following two qubit evolution (in the representation with the basis$\{|11\rangle, |10\rangle, |01\rangle, |00\rangle\}$

$$\hat{U} = e^{-i\hat{H}_I t/\hbar} = \begin{pmatrix} 1 & 0 & 0 & 0 \\ 0 & \cos\xi & -i\sin\xi & 0 \\ 0 & -i\sin\xi & \cos\xi & 0 \\ 0 & 0 & 0 & 1 \end{pmatrix},\ \xi = tC_{ul}^{xx}/\hbar. \tag{26}$$

This is the typical two-qubit i-SWAP gate. With such an universial gate, assisted by arbitrary rotations of single qubits, any quantum computing network could be constructed [1].

We now discuss the possible leakages due to Coulomb interaction, i.e., the electrons may populate the bound states outside the computational basis. Without loss of the generality, the third bound state $|2\rangle$ of each electrons is also considered. Therefore, we need to discuss the two-qubit dynamics within a nine-dimensional subspace $\Xi = \{|00\rangle, |01\rangle, |10\rangle, |11\rangle, |02\rangle, |20\rangle, |12\rangle, |21\rangle, |22\rangle\}$, and the Hamiltonian of the two-qubit system should be written as a 9×9 matrix. However, one can easily check (in the interaction picture under the usual rotating-wave approximation) that, there are just three invariant subspaces including the computational basis: $(\mathrm{i})\mathrm{Im}_1 = \{|00\rangle\}, (\mathrm{ii})\mathrm{Im}_2 = \{|01\rangle, |10\rangle\}$, and $(\mathrm{iii})\mathrm{Im}_3 = \{|02\rangle, |11\rangle, |20\rangle\}$. This means that the possible leakage only takes place in the third invariant subspace, i.e., the states $|20\rangle$ and $|02\rangle$ might be populated during the two-qubit operation. The Hamiltonian in such an invariant subspace can be expressed as

$$\hat{H}_3 = \begin{pmatrix} A_1 & -2z_l^{01}z_u^{21}e^{-it(\omega_l^{10}-\omega_u^{21})} & -2z_l^{02}z_u^{20}e^{-it(\omega_l^{20}-\omega_u^{20})} \\ -2z_l^{10}z_u^{12}e^{it(\omega_l^{10}-\omega_u^{21})} & A_2 & -2z_l^{12}z_u^{10}e^{-it(\omega_l^{21}-\omega_u^{10})} \\ -2z_l^{20}z_u^{02}e^{it(\omega_l^{20}-\omega_u^{20})} & -2z_l^{21}z_u^{01}e^{it(\omega_l^{21}-\omega_u^{10})} & A_3 \end{pmatrix}, \tag{27}$$

with the frequencies $\omega_k^{mn} = (E_m^k - E_n^k)/\hbar$, $m, n = 0, 1, 2$; $k = u, l$, and

$$\begin{aligned} A_1 &= (z_l^{00})^2 + z_l^{01}z_l^{10} + z_l^{02}z_l^{20} + (z_u^{22})^2 + z_u^{20}z_u^{02} + z_u^{21}z_u^{12} - 2z_l^{00}z_u^{22}, \\ A_2 &= (z_l^{11})^2 + z_l^{10}z_l^{01} + z_l^{12}z_l^{21} + (z_u^{11})^2 + z_u^{10}z_u^{01} + z_u^{12}z_u^{21} - 2z_l^{11}z_u^{11}, \\ A_3 &= (z_l^{22})^2 + z_l^{20}z_l^{02} + z_l^{21}z_l^{12} + (z_u^{00})^2 + z_u^{01}z_u^{10} + z_u^{02}z_u^{20} - 2z_l^{22}z_u^{00}. \end{aligned}$$

The dynamics determined by this Hamiltonian can be numerically solved and the time-dependent populations of the involved bound states are shown in Fig. 5, wherein the involved parameters are calculated as: $z_u^{22} = -5.548 \times 10^{-1}$ μm, $z_u^{02} = z_u^{20} = 1.9787 \times 10^{-3}$ μm, $z_u^{21} = z_u^{12} = 8.1606 \times 10^{-2}$ μm; $z_l^{22} = -4.287 \times 10^{-1}$ μm, $z_l^{02} = z_l^{20} = -2.4678 \times 10^{-4}$ μm, $z_l^{21} = z_l^{12} = -3.6634 \times 10^{-3}$ μm; and $\omega_l^{10} - \omega_u^{21} = 3.9519 \times 10^{10}$ rad/s, $\omega_l^{21} - \omega_u^{10} = 6.9369 \times 10^{11}$ rad/s, $\omega_l^{20} - \omega_u^{20} = 7.3321 \times 10^{11}$ rad/s. Fig. (5a) shows that the population transfer between the computational basis $|01\rangle$ and $|10\rangle$ could be implemented by properly setting the duration of the Coulomb interaction between the electrons in different MQDs. Furthermore, it is seen from Fig. (5b) that, the leakages of the populations from the computational basis $|11\rangle$ are relatively weak, e.g., the probabilities transferred to the state $|02\rangle$ are less than 10% and to the state $|20\rangle$ are really negligible. In fact,

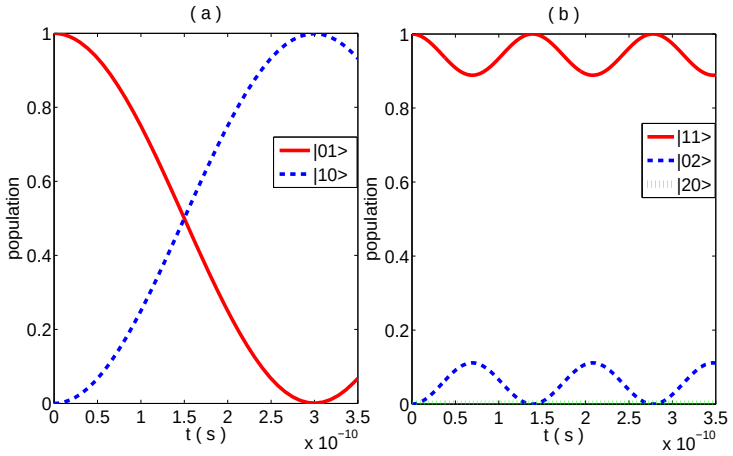

FIG. 5: (Color online) Population evolutions of two coupled qubits during an i-SWAP gate operation. (a) The population transfers between the computational basis $|10\rangle$ and $|01\rangle$, and (b) Population of the computational basis $|11\rangle$ versus the duration. It is seen that the leakages of the population from the state $|11\rangle$ to the states $|20\rangle$ and $|02\rangle$ are relatively weak. In these numerical calculations, the parameter d which represents the distance of the two Q1DCs is typically set as 1.1 μm, and the others are the same as those used in Figs. 1-3.

weaker leakages could be achieved by decreasing the value of the parameter $z(\neq 0)$. Also, we have numerically checked that the adiabatic changes of the levels do not significantly deduce the unwanted leakages. In this sense, the desirable i-SWAP gate between the MQDs in different channels can be implemented and the relevant leakages could be effectively suppressed.

V. DISCUSSIONS AND CONCLUSIONS

Readout of the qubits is another crucial tasks in quantum computing. In Barnes et al's scheme [14], the flying qubit is encoded by the spin-states of the electrons in the MQDs and its readout is implemented by using the usually magnetic Stern-Gerlach effect. In our proposal the flying qubit is encoded by the lowest two levels of the electron in the moving trapped potential. These levels are theoretically steady but still exist weak tunnelings. Thus, by detecting the tunnelings of the moving electron from the trapped potential, one can achieve the qubit readouts. This is because that the tunneling rates of electron in either the state $|0\rangle$ or the state $|1\rangle$ should be different and thus could be distinguished individually. In fact, these tunneling-measurements have been realized in the recent experiment [18]. There, another channel is introduced to detect the tunnelings of the electrons in the MQDs across the computational channels. Physically, the flying

electron in the state $|1\rangle$ should yield significantly-high probability of tunneling to the detecting channel, and thus decrease the current $I_{\rm top}$ flowing along the computational channel. While, if the flying electron in the ground level $|0\rangle$, then the probability of tunneling out should be obviously small and thus $I_{\rm top}$ should be almost unchanged. Stronger tunnelings are also possible, if the flying qubit is excited for leakage. This can be achieved by applying a resonant pulse to excite the electron staying at the computational basis $|0\rangle$ (or $|1\rangle$) to the higher level (e.g., the state $|2\rangle$) with significantly-bigger tunneling-probabilities [26]. By this way, flying qubit staying at $|0\rangle$ or $|1\rangle$ could be more robustly detected.

Another challenge for realizing our proposal is how to hold only one electron in a MQD across the computational channel. Initially, many electrons can be captured by the SAWs from the source region of 2DEG; the number of electrons residing in the minima of SAWs depend on the size of the formed quantum dot. Note that the static potential generated by the split-gate is fixed, but the depth and the curvature of the MQD vary with the time during the MQD moving along the channel. When the size of the dot becomes smaller, electrons captured from the source are ejected from the dot and let a few ones be still trapped by the potential. By suitably controlling the relevant parameters, e.g., the power of the SAW and the split-gate voltage, only one electron could reside in a MQD for realizing the desirable flying qubit [21]. Also, the thermal excitations of the present qubit can be safely neglected as the experimental temperature is sufficiently low, so the captured electron can be kept in its ground state except it is driven by external field. Finally, as in all the other solid-state quantum computing candidates, decoherence in the present flying qubit is also an open problem and would be discussed in future.

In summary, we have put forward an approach to implementing quantum computation with the energy levels of the electrons trapped in the MQDs. The idea involves the capture of electrons from a 2DEG by the SAWs to form the potentials for trapping a single electron. Each SAW may capture many electrons from the 2DEG source, but we can make only one electron reside in the minimum of the SAW by tuning the surface split-gate to change the barrier height, that forces the excessive electrons to tunnel out from the quantum dot. By numerical method, we have known that few adiabatic levels of each electron could be formed in a MQD, and the lowest two ones are utilized to encode a flying qubit. We have shown how to implement the Rabi oscillations with the flying qubit for performing single-qubit operation. A two-qubit gate, i.e., i-SWAP gate, has also be constructed by using the Coulomb interaction of the electrons in different MQDs across the nearest-neighbor computational channels. In principle, our proposal can be extended to the

system including N qubits by integrating an array of N Q1DCs.

Acknowledgments

This work was supported in part by the National Science Foundation grant No. 10874142, 90921010, and the National Fundamental Research Program of China through Grant No. 2010CB923104, and the Fundamental Research Funds for the Central Universities No. SWJTU09CX078. We thank Prof. J. Gao for encouragements and Dr. Adam Thorn for kind helps.

[1] S. Lloyd, Science **261**, 5128 (1993).

[2] P. W. Shor, Proceedings of the 35th Annual Symposium on Foundations of Computer Science (IEEE Computer Press,Los Alamitos, 1994), p. 124.

[3] A. S. Parkins, P. Marte and P. Zoller, Phys. Rev. Lett. **71**, 3095 (1993).

[4] T. Pellizzari, S. A. Gardiner, J. I. Cirac and P. Zoller, Phys. Rev. Lett. **45**, 3788 (1995).

[5] See, e.g., J. I. Cirac and P. Zoller, Phys. Rev. Lett. **74**, 4091 (1995); L. F. Wei, S. Y. Liu, and X. L. Lei, Phys. Rev. A **65**, 062316 (2002).

[6] N. A. Gershenfeld and I. L. Chuang, Science **275**, 350-356 (1997).

[7] D. Bouwmeester, J. W. Pan, M. Daniell, H. Weinfurter and A. Zeilinger, Phys. Rev. Lett. **82**, 1345 (1999).

[8] Y. H. Kim, S. P. Kulik, M. V. Cekhova, W. P. Grice and Y. Shih, Phys. Rev. A **67**, 010301 (2003).

[9] D. Loss and D. P. DiVincenzo, Phys. Rev. A **57**, 120 (1998).

[10] K. R. Brown, D. A. Lidar and K. B. Whaley, Phys. Rev. A **65**, 012307 (2001).

[11] See, e.g., Y. Makhlin, G. Schön, and A. Shnirman, Rev. Mod. Phys. **73**, 357 (2001); L. F. Wei, Yu-xi Liu, and Franco Nori, Phys. Rev. B **71**, 134506 (2005).

[12] J. M. Shilton, V. I. Talyanskii, M. Pepper, D. A. Ritchie, J. E. F. Frost, C. J. V. Ford, C. G. Smith and G. A. C. Jones, J. Phys. Condens. Matter **8**, L531 (1996).

[13] V. I. Talyanskii, J. M. Shiltion, M. Pepper, C. G. Smith, C. J. B. Ford, E. H. Linfield, D. A. Ritchie, and G. A. C. Jones, Phys. Rev. B **56**, 15180 (1997).

[14] C. H. W. Barnes, J. M. Shilton, and A. M. Robinson, Phys. Rev. B **62**, 8410 (2000).

[15] S. Furuta, C. H. W. Barnes, and C. J. L. Doran, Phys. Rev. B **70**, 205320 (2004).

[16] R. Rodriquez, D. K. L. Oi, M. Kataoka, C. H. W. Barnes, T. Ohshima and A. K. Ekert, Phys. Rev. B **72**, 085329 (2005).

[17] P. Bordone, A. Bertoni, MRosini, S. Reggiani and C. Jacoboni, Semicond. Sci. Technol. **19**, S412 (2004).

[18] M. Kataoka, M. R. Astley, A. L. Thorn, D. K. L. Oi, C. H. W. Barnes, C. J. B. Ford, D. Anderson, G. A. C. Jones, I. Farrer, D. A. Ritchie, and M. Pepper, Phys. Rev. Lett. **102**, 156801 (2009).

[19] J. Cunningham, V. I. Talyanskii, J. M. Shilton, M. Pepper, M. Y. Simmons and D. A. Ritchie, Phys. Rev. B **60**, 4850 (1999).

[20] M. Kataoka, R. J. Schneble, A. L. Thorn, C. H. W. Branes, X. J. V. Ford, D. Anderson, G. A. C. Jones, I. Farrer, D. A. Ritchie, and M. Pepper, Phys. Rev. Lett. **98**, 046801 (2007).

[21] A. M. Robinson and C. H. W. Barnes, Phys. Rev. B **63**, 165418 (2001).

[22] G. Gumbs, G. R. Aĭzin and M. Pepper, Phys. Rev. B **60**, 13954 (1999).

[23] G. Gumbs and Y. Abranyos, Phys. Rev. A **70**, 050302 (2004).

[24] G. R. Aĭzin, G. Gumbs, and M. Pepper, Phys. Rev. B **58**, 10589 (1998).

[25] S. L. Zhu and Z. D. Wang, Phys. Rev. Lett. **89**, 097902 (2002).

[26] M. R. Astley, M. Kataoka, C. J. B. Ford, C. H. W. Barnes, D. Anderson, G. A. C. Jones, I. Farrer, D. A. Ritchie, and M. Pepper, Phys. Rev. Lett. **99**, 156802 (2007).